Transportation Research Part C 109 (2019) 79–94

Contents lists available at ScienceDirect

Transportation Research Part C

journal homepage: www.elsevier.com/locate/trc

An extension of Newell's simplified kinematic wave model to account for first-in-first-out violation: With an application to vehicle trajectory estimation

Adrian Rey[a], Wen-Long Jin[b,*], Stephen G. Ritchie[c]

[a] Institute of Transportation Studies, 4000 Anteater Instruction and Research Bldg, University of California, Irvine, CA 92697-3600, United States
[b] Department of Civil and Environmental Engineering, California Institute for Telecommunications and Information Technology, Institute of Transportation Studies, 4000 Anteater Instruction and Research Bldg, University of California, Irvine, CA 92697-3600, United States
[c] Department of Civil and Environmental Engineering, Institute of Transportation Studies, 4000 Anteater Instruction and Research Bldg, University of California, Irvine, CA 92697-3600, United States

ARTICLE INFO

Keywords:
Newell's simplified kinematic wave model
Trajectory estimation
Eulerian and Lagrangian traffic data
First-In-First-Out (FIFO) violation
Vehicle order
Next Generation Simulation (NGSIM) dataset.

ABSTRACT

Newell's simplified kinematic wave model has been widely used in studying traffic dynamics in a road network. However, it cannot account for First-In-First-Out violation among vehicles on multi-lane roads. In this study, we present an extension of the model in the Lagrangian coordinates. In particular, we define a new variable of a vehicle's order as its corresponding cumulative flows at different times and locations. The new kinematic wave model is consistent at the aggregate level with Newell's simplified kinematic wave model, but allows for FIFO violation among individual vehicles.

Based on the new model, we then present two algorithms to estimate vehicles' trajectories from Eulerian data (cumulative flows provided by loop detectors) and Lagrangian data (the vehicle's entry and exit times provided by reidentification technologies) at two boundaries of a road segment. In the first algorithm, we assume that vehicles follow the First-In-First-Out (FIFO) principle on a multi-lane road, and their orders are constant and equal the average of the entry and exit orders; in the second algorithm, we introduce a linear order-changing model to interpolate a vehicle's orders at different times according to its entry and exit times. With Next Generation Simulation (NGSIM) datasets, we demonstrate that both algorithms are effective, but the second one, with an estimation error of around 10%, greatly outperforms the first one, with an estimation error of around 13%. This verifies the advantage of incorporating FIFO violation in the new model.

1. Introduction

In Newell (1993), a simplified kinematic wave model was presented for modeling traffic dynamics in a road network. This model is a reformulation of the LWR model (Lighthill and Whitham, 1955; Richards, 1956), by changing the state variable from traffic densities to cumulative flows. Thus Newell's simplified kinematic wave model is the Hamilton-Jacobian equation of the LWR model, and the former has many theoretical and computational advantages for studying network traffic flow (See (Jin, 2015) and references therein). In Jin (2017), Yan and Jin (2017), Jin and Yan (2019), it was theoretically and empirically shown that First-In-First-Out

* Corresponding author.
E-mail address: wjin@uci.edu (W.-L. Jin).

https://doi.org/10.1016/j.trc.2019.10.005
Received 22 July 2018; Received in revised form 9 October 2019; Accepted 9 October 2019

(FIFO) violation among vehicles on multi-lane roads can be captured by unifiable multi-commodity kinematic wave model, in which the total traffic follows the traditional LWR model, but vehicles of different commodities can travel at different speeds at the same time and location. However, Newell's simplified kinematic wave model cannot account for such FIFO violation directly, even though FIFO violation was demonstrated to be prevalent in simulations (Jin et al., 2006) and real-world observations (Jin and Li, 2007).

In this study we present an extension of Newell's simplified kinematic wave model in the Lagrangian coordinates to include FIFO violation. In the original Newell's model, also referred to as the three-detector method (Daganzo, 1997, Section 4.4), the cumulative flow at a point inside a road segment can be calculated as the minimum of two translated curves from the cumulative flows at the upstream and downstream boundaries. Thus the original Newell's model is formulated in the Eulerian coordinates, with the time and location as independent variables. In contrast, the new model is in the Lagrangian coordinates, and vehicles' locations are determined by the boundary cumulative flows, with the time and vehicle ID as independent variables. Note that the new model still has Eulerian boundary conditions at the two segment boundaries; this is also different from existing kinematic wave models in the Lagrangian coordinates, i.e., car-following models, whose boundary conditions with leaders' locations are also Lagrangian (Newell, 2002; Laval and Leclercq, 2013; Jin, 2016). In this sense, we present a novel kinematic wave model in the Lagrangian coordinates but under Eulerian boundary conditions.

More importantly, the new model can explicitly accommodate overtakings and FIFO violation of vehicles. This is realized by introducing a new variable, vehicle order: a vehicle's order at a time is measured by the moment's cumulative flow at the vehicle's location. If all vehicles follow the FIFO principle, a vehicle's order is time-independent and equals the cumulative flow. However, when the FIFO principle is violated, a vehicle's order varies with time. Thus the new model is different from existing car-following models, including Newell's simplified car-following mode (Newell, 2002), where the FIFO principle is always satisfied.

Such a new model is of not only theoretical but also practical interests, as it can be readily applied to estimate vehicles' trajectories on multi-lane roads. Real time traffic control is essential to improve the performance of the overall traffic system and to maximize the benefits of users and society. The better the information about current traffic states, the better decisions and strategies can be made. Estimating trajectories is the best way to have a complete picture of the traffic state in a road network, since it provides valuable information to deduce all other traffic variables and the congestion level. Besides, having vehicle trajectories over a freeway link is useful to develop other important applications, such as more accurate estimations of vehicle emissions, which are determined by not only the average speeds but also the acceleration rates, as well as safer and more efficient guidance of autonomous vehicles in a traffic stream.

In the literature many methods have been developed to estimate such aggregate traffic states as the density, speed, and flow rate (Seo et al., 2017). However, there are very few existing studies on estimating vehicle trajectories. The methods used for this purpose vary from processing the images recorded by video cameras to more complex systems merging global-positioning-system (GPS) data with Kalman Filtering and geographic-information-system (GIS) data (Barrios and Motai, 2011). In the middle, several different approaches can be found, such as computer vision algorithms using monocular vision (Ponsa and Lopez, 2007) or other estimation strategies with GPS or radar devices. Apart from these, there are also some studies that deal with the problem from the traffic flow theory perspective. For example, the study in Coifman (2002) presented an interesting new method to solve the problem of estimating vehicle trajectories; the idea was to develop an estimation of link travel times and vehicle trajectories from data collected by dual loop detectors, without requiring any new hardware. In Mehran et al. (2012), a data fusion method based on the kinematic wave theory is proposed to reconstruct vehicle trajectories from loop detector and probe vehicle data, taking into account of entering and exiting vehicles, on a signalized road segment. In Jiang et al. (2017), travel speeds of probe vehicles are estimated with detailed GPS data and loop detector data, and virtual vehicle trajectories are constructed accordingly. In Li et al. (2019), vehicles' trajectories are constructed iteratively with Newell's simplified car-following model and used to cross-validate vehicle speeds. Other methods have been proposed to reconstruct vehicle trajectories on signalized roads in Yang et al. (2011), Sun and Ban (2013), Sun et al. (2015), Wan et al. (2016), Mo et al. (2017). All these methods assume the First-In-First-Out (FIFO) principle, which limits their applications to single-lane roads without systematic overtakings.

To the best of our knowledge, however, there exists no method that explicitly takes into account of FIFO violation when estimating vehicle trajectories on multilane facilities. A major motivation of developing the new model in this study is to more accurately estimate individual vehicle trajectories from both Eulerian and Lagrangian data by incorporating FIFO violation on a multilane freeway segment. In particular, the Eulerian data are cumulative flows from loop detectors, and the Lagrangian data are vehicles' orders from vehicle reidentification technologies, including video cameras, AVI (automatic vehicle identification) tags, and loop detectors (Sun et al., 1999; Jeng, 2007). Various applications of vehicle reidentification technologies have been developed for travel time estimation (Coifman and Cassidy, 2002), system performance evaluation (Jeng, 2007; Oh et al., 2005), and origin-destination demand estimation (Oh et al., 2002). Here we consider a homogeneous road segment, on which the number of lanes, speed limits, and other traffic characteristics are the same at different locations, and a general traffic network can be modeled as combinations of individual segments with a single entry and exit. With the reidentification technologies, a vehicle's orders at the two boundaries can be detected. If assuming that a vehicle's order linearly change with time, then we can find the vehicle order at any time. Then we can estimate its location at a time from the new formulation of Newell's simplified kinematic wave model. We test the performance of the new estimation method with the NGSIM datasets (USDOT, 2008). The model's parameters, such as the free flow speed, shock wave speed and jammed density, as well as the initial state (i.e. initial number of vehicles inside the segment), have been calibrated with the same Eulerian and Lagrangian datasets in Sun et al. (2017).

A list of notations is provided in Table 1.

The rest of the paper is organized as follows. In Section 2, we review Newell's simplified kinematic wave model and present two lemmas for its properties. In Section 3, we define vehicles' orders and present an extension of Newell's simplified kinematic wave

Table 1
Notations

$F(t)$	The **observed** cumulative count at the upstream from 0 to t
$G(t)$	The **observed** cumulative count at the downstream from 0 to t
N_0	The initial number of vehicles within the segment
$N(x, t)$	The cumulative flow at location x and time t
V	Free-flow speed
W	Shock-wave speed in congested traffic
K	Jam density
$X_i(t)$	Location of vehicle i at time t
$\theta_i(t)$	Order of vehicle i at time t
Δt	Time step size
l	Length of the road segment
r_i	Entrance time of vehicle i
s_i	Exit time of vehicle i

model by incorporating vehicles' orders in the Lagrangian coordinates. In Section 4, we present two algorithms for estimating vehicles' trajectories from Eulerian and Lagrangian data: the first assuming the FIFO principle and the second not. In Section 5, we use the NGSIM data to demonstrate the advantages of the model with FIFO violation. We conclude the whole study in Section 6.

2. Newell's simplified kinematic wave model and its properties

Let's consider a homogeneous road segment of length l from $x = 0$ to $x = l$. At the aggregate level, traffic conditions on the road segment can be perfectly described using the cumulative flows, $N(x, t)$, which is also referred to as the Moskowitz function (Moskowitz, 1965). Here $N(x, t)$ is the number of vehicles passing x at t after a reference vehicle. The flow-rate is

$$q\left(x, t\right) = \frac{\partial N(x, t)}{\partial t}, \tag{1}$$

and the density is

$$k\left(x, t\right) = -\frac{\partial N(x, t)}{\partial x}. \tag{2}$$

2.1. Newell's model

The Lighthill-Whitham-Richard (LWR) kinematic wave model (Lighthill and Whitham, 1955) uses a partial differential equation to describe the evolution of traffic conditions in terms of density, flow-rate, and speed:

$$\frac{\partial k(x, t)}{\partial t} + \frac{\partial \phi(k(x, t))}{\partial x} = 0, \tag{3}$$

where $k(x, t)$ is traffic density, and $q(x, t) = \phi(k(x, t))$ is the fundamental diagram (Greenshields, 1935).

In Newell's study (Newell, 1993), he pointed out that the kinematic wave model could be streamlined with a triangular fundamental diagram using cumulative flow $N(x, t)$ as a state variable, leading to a simpler formulation of the problem. That is, the LWR model, (3), is equivalent to the following Hamilton-Jacobi equation (Evans, 1998, Chapter 3):

$$\frac{\partial N(x, t)}{\partial t} - \phi\left(-\frac{\partial N(x, t)}{\partial x}\right) = 0. \tag{4}$$

Further in Newell's model, a triangular flow-density relation is used (Munjal et al., 1971; Haberman, 1977; Newell, 1993):

$$\phi(k) = \min\{Vk, W{\cdot}(K - k)\}, \tag{5}$$

where V is the free-flow speed, $-W$ the shockwave speed in congested traffic, and K the jam density. This diagram is represented in Fig. 1, where the critical density $k_C = \frac{W}{V+W}K$, and the capacity $C = Vk_C$.

Without loss of generality, we denote the vehicle at $x = l$ and $t = 0$ as the reference vehicle. As shown in Table 1, we denote the observed cumulative count (number of vehicles) at the downstream boundary from 0 to t by $G(t)$; i.e.,

$$G(t) = N(l, t). \tag{6}$$

We also denote the observed cumulative count at the upstream boundary from 0 to t by $F(t)$, which is different from $N(0, t)$ due to the presence of an initial number of vehicles within the segment, N_0. Thus

$$F(t) + N_0 = N(0, t). \tag{7}$$

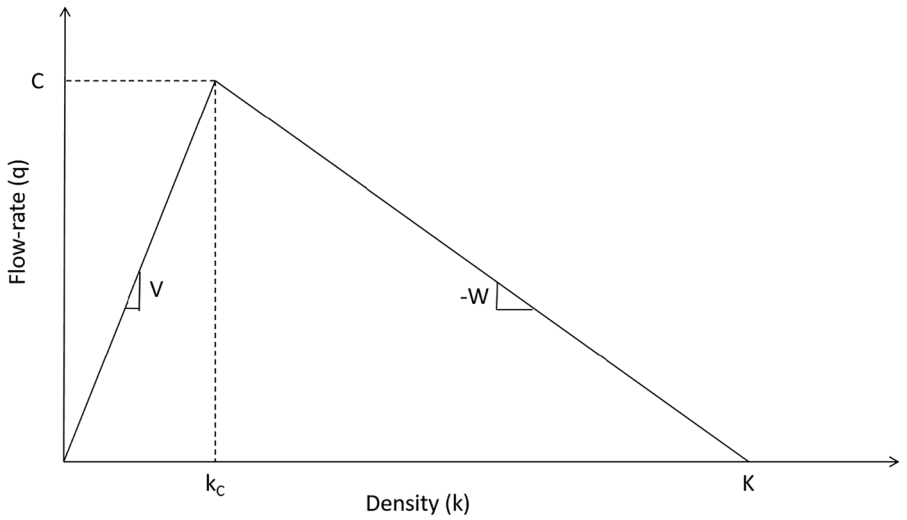

Fig. 1. Triangular fundamental diagram.

Here $F(0) = G(0) = 0$. Since the upstream detector does not count the vehicles entered the segment before $t = 0$, N_0 is not available but can be estimated from $F(t)$, $G(t)$, and some vehicles' entry and exit times using the method developed in Sun et al. (2017). Note that the cumulative flow $N(x, t)$ is defined with respect to a reference vehicle and can be negative; but the cumulative counts (numbers), $F(t)$ and $G(t)$, are defined with respect to $t = 0$ and non-negative.

In Newell's simplified kinematic wave model (Newell, 1993), the cumulative flow at any location on the road $x \in [0, l]$ and time $t > 0$ can be calculated from cumulative flows at both boundaries at a road segment with the following variational principle (Daganzo, 2005):

$$N\left(x, t\right) = \min\left\{F\left(t - \frac{x}{V}\right) + N_0,\ G\left(t - \frac{l - x}{W}\right) + \left(l - x\right)K\right\}. \tag{8}$$

This equation means that the cumulative flow is either determined by the upstream conditions (the first term in the equation) or the downstream conditions (the second term in the equation). Geometrically, $N(x, t)$ is a surface in the (x, t)-coordinate and the lower envelope of two surfaces: $F(t - \frac{x}{V}) + N_0$, and $G(t - \frac{l-x}{W}) + (l - x)K$. In Jin (2015), it was shown that (8) is a simplification of the Hopf-Lax formula for the Hamilton-Jacobi equation, (4), with the triangular fundamental diagram, (5), when the initial traffic condition does not contain a transonic rarefaction wave.

In this study, we assume that the cumulative numbers of vehicles, $F(t)$ and $G(t)$, are collected from loop detectors at both boundaries of a road segment. In addition, the partial trajectories (i.e. entry/exit times) of a number of vehicles can be obtained through vehicle reidentification technologies. In Sun et al. (2017), (8) was used to estimate the initial number of vehicles, N_0, and parameters, K and W, in congested traffic from observed $F(t)$, $G(t)$, and entry and exit times of a subset of vehicles. Based on the aforementioned study, we assume that all of these parameters are given and estimate the trajectory of one or more vehicles.

2.2. Properties

Let's first introduce the notation $N_1(x, t)$ to refer to the uncongested part of the Newell's equation, (8), and $N_2(x, t)$ to refer to the congested part. We have

$$N_1\left(x, t\right) = F\left(t - \frac{x}{V}\right) + N_0, \tag{9}$$

and

$$N_2\left(x, t\right) = G\left(t - \frac{l - x}{W}\right) + \left(l - x\right)K. \tag{10}$$

Thus (8) can be written as

$$N(x, t) = \min\{N_1(x, t), N_2(x, t)\}. \tag{11}$$

Clearly both $N_1(x, t)$ and $N_2(x, t)$ are non-decreasing in t, as both $F(t)$ and $G(t)$ are non-decreasing. Without loss of generality, we assume that they are strictly increasing; i.e., the boundary flow-rates are always positive. For simplicity, we also assume that both $N_1(x, t)$ and $N_2(x, t)$ are differentiable with respect to x and t; i.e., $F(t)$ and $G(t)$ are differentiable. In the following lemma, we

demonstrate that they are non-increasing in x.

Lemma 2.1. *At a time instant, both $N_1(x, t)$ and $N_2(x, t)$ are non-increasing in x, and their partial derivatives satisfy the following relation:*

$$-K \leqslant \frac{\partial N_2(x,t)}{\partial x} \leqslant -k_C \leqslant \frac{\partial N_1(x,t)}{\partial x} \leqslant 0. \tag{12}$$

This is equivalent to saying that the density is under-critical (between 0 and k_C) along $N_1(x, t)$ and over-critical (between k_C and K) along $N_2(x, t)$.

Proof. In the triangular fundamental diagram, (5), we have

$$C = Vk_C = W(K - k_C).$$

Besides, the terms $F'(t)$ and $G'(t)$ correspond to the road's entry and exit flow-rates, respectively, so they have to satisfy

$$0 \leqslant \min\{F'(t), G'(t)\} \leqslant \max\{F'(t), G'(t)\} \leqslant C.$$

Therefore, we can write

$$\begin{aligned}
&\tfrac{\partial N_1(x,t)}{\partial x} = F'(t - \tfrac{x}{V})\cdot(-\tfrac{1}{V}) \leqslant 0,\\
&\tfrac{\partial N_1(x,t)}{\partial x} = F'(t - \tfrac{x}{V})\cdot(-\tfrac{1}{V}) \geqslant -\tfrac{C}{V} = -k_C,\\
&\tfrac{\partial N_2(x,t)}{\partial x} = G'(t - \tfrac{l-x}{W})\cdot(\tfrac{1}{W}) - K \geqslant -K,\\
&\tfrac{\partial N_2(x,t)}{\partial x} = G'(t - \tfrac{l-x}{W})\cdot(\tfrac{1}{W}) - K \leqslant \tfrac{C}{W} - K = -k_C.
\end{aligned}$$

Thus (12) is satisfied: both $N_1(x, t)$ and $N_2(x, t)$ decrease in x, but the latter's absolute rate of change is larger. □

Lemma 2.2. *At any time instant t, the road segment $x \in [0, l]$ can be divided into three sub-segments, as shown in Fig. 2:*

1. For $x \in [0, a)$, $N_1(x, t) < N_2(x, t)$, and $N(x, t) > N(a, t)$. In this sub-segment, traffic is strictly under-critical.
2. For $x \in [a, b]$, $N_1(x, t) = N_2(x, t)$, and $N(x, t) \in [N(b, t), N(a, t)]$. In this sub-segment, traffic is critical.
3. For $x \in (b, l]$, $N_1(x, t) > N_2(x, t)$, and $N(x, t) < N(b, t)$. In this sub-segment, traffic is strictly over-critical.*Two special cases are when $a = b = 0$ when the whole road is congested or $a = b = l$ when the whole road is uncongested.*

Proof. At the entry and exit points $x = 0$ and $x = l$ we know by the definition that

$$\begin{aligned}
&N_1\left(0, t\right) = F(t) + N_0 = \min\left\{F(t) + N_0, G(t - \tfrac{l}{W}) + Kl\right\} \leqslant G\left(t - \tfrac{l}{W}\right) + Kl = N_2\left(0, t\right),\\
&N_2\left(l, t\right) = G(t) = N\left(l, t\right) = \min\left\{F(t - \tfrac{l}{V}) + N_0, G(t)\right\} \leqslant F\left(t - \tfrac{l}{V}\right) + N_0 = N_1\left(l, t\right).
\end{aligned}$$

Taking into account that both $N_1(x, t)$ and $N_2(x, t)$ are continuous functions, we can state that at t

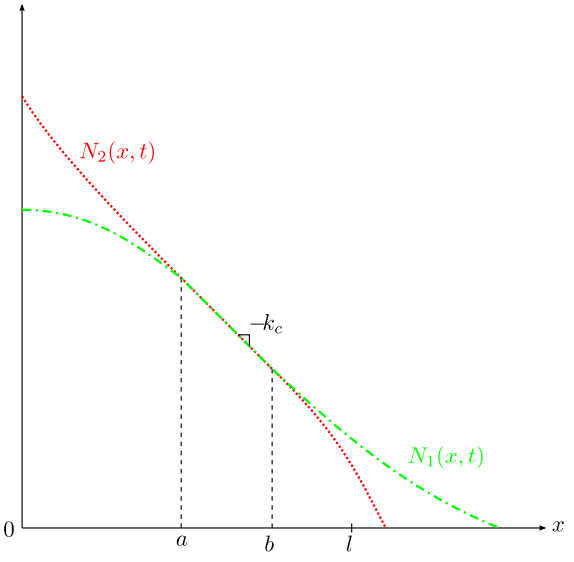

Fig. 2. Illustration of three sub-segments of a road at a fixed t in Newell's simplified kinematic wave model.

$$\exists\ [a, b] \subseteq [0, l] | \{\forall\ x \in [a, b],\ N_1(x, t) = N_2(x, t)\}.$$

That is $N_1(x, t)$ and $N_2(x, t)$ overlap for $x \in [a, b]$. Note that in general we will have $a = b$ and only one intersection point, but it could be possible that $N_1(x, t)$ and $N_2(x, t)$ had a whole interval of common points, since their decreasing rates can be equal when $\frac{\partial N_1(x,t)}{\partial x} = \frac{\partial N_2(x,t)}{\partial x} = -k_C$ (see Eq. (12)). Thus we can separate the segment into three sub-segments as stated in Lemma 2.2. □

We denote $X_1(n, t)$ and $X_2(n, t)$ as the respective inverse functions of $N_1(x, t)$ and $N_2(x, t)$; i.e., $X_1(n, t)$ satisfies

$$N_1\left(X_1\left(n, t\right), t\right) = F\left(t - \frac{X_1(n, t)}{V}\right) + N_0 = n, \tag{13}$$

and $X_2(n, t)$ satisfies

$$N_2\left(X_2\left(n, t\right), t\right) = G\left(t - \frac{l - X_2(n, t)}{W}\right) + \left(l - X_2\left(n, t\right)\right)K = n. \tag{14}$$

Without loss of generality, here we assume that $\frac{\partial N_1(x,t)}{\partial x} < 0$, which implies that $\frac{\partial N_2(x,t)}{\partial x} < 0$ from Lemma 2.1. Thus both $N_1(x, t)$ and $N_2(x, t)$ are strictly decreasing, and $X_1(n, t)$ and $X_2(n, t)$ are well-defined and can be calculated from n as well as the boundary cumulative flows. In the following, we can then obtain an equivalent formulation of Newell's model in (11) in terms of vehicles' locations.

Theorem 2.3. *Newell's model in (11) is equivalent to*

$$X(n, t) = \min\{X_1(n, t), X_2(n, t)\}, \tag{15}$$

where $X(n, t)$ is the location of cumulative flow n at t.

Proof. According to Lemma 2.2, we can prove (15) in the three sub-segments as follows:

1. When $0 \leqslant x < a$ and $n > N(a, t)$, $N_1(x, t) < N_2(x, t)$, and $X_1(n, t) < X_2(n, t)$. Thus $N(X(n, t), t) = N_1(X(n, t), t) = n$, and $X(n, t) = X_1(n, t) = \min\{X_1(n, t), X_2(n, t)\}$.
2. When $a \leqslant x \leqslant b$ and $N(b, t) \leqslant n \leqslant N(a, t)$, $N_1(x, t) = N_2(x, t)$, and $X_1(n, t) = X_2(n, t)$. Thus $N(X(n, t), t) = N_1(X(n, t), t) = N_2(X(n, t), t) = n$, and $X(n, t) = X_1(n, t) = X_2(n, t) = \min\{X_1(n, t), X_2(n, t)\}$.
3. When $b < x \leqslant l$ and $n < N(b, t)$, $N_1(x, t) > N_2(x, t)$, and $X_1(n, t) > X_2(n, t)$. Thus $N(X(n, t), t) = N_2(X(n, t), t) = n$, and $X(n, t) = X_2(n, t) = \min\{X_1(n, t), X_2(n, t)\}$.

Thus (15) is true in all three cases. These three scenarios are also illustrated in Fig. 2. □

Note that (15) can be also proved by applying the Hopf-Lax formula for the following Hamilton-Jacobi equation of the LWR model in the Lagrangian coordinates (Laval and Leclercq, 2013),

$$\frac{\partial X(n, t)}{\partial t} = \min\left\{V, W\left(-K\frac{\partial X(n, t)}{\partial n} - 1\right)\right\},$$

subject to the following boundary conditions:

$$X(F(t) + N_0, t) = 0, \quad X(G(t), t) = l.$$

That is, (15) is still valid even if $F(t)$ and $G(t)$ are non-differentiable with the existence of shock waves. But for simplicity we omit such a proof. The interested reader can verify this by extending the relevant arguments in Laval and Leclercq (2013) and Jin (2015).

3. An extension of Newell's simplified kinematic wave model to account for FIFO violation

In this section we present an extension of Newell's model in the Lagrangian coordinates, where a vehicle's ID and time are independent variables. We denote vehicle i's location by $X_i(t)$, and its entry and exit times by r_i and s_i respectively. Then, for vehicle i, we have $X_i(r_i) = 0$ and $X_i(s_i) = l$, where r_i and s_i are respectively the entry and exit times of vehicle i. For a time between the entry and exit times, $X_i(t)$ is to be estimated.

3.1. A new variable of vehicle order

We denote vehicle i's order at t by $\theta_i(t)$, which is defined as the corresponding cumulative flow at $X_i(t)$ and t. That is,

$$\theta_i(t) = N(X_i(t), t). \tag{16}$$

That is, vehicle i is the $\theta_i(t)$-th vehicle passing $X_i(t)$, after a reference vehicle. Therefore,

$$X_i(t) = X(\theta_i(t), t). \tag{17}$$

Thus, if $X_i(t) < X_j(t)$ for vehicles i and j, then $\theta_i(t) > \theta_j(t)$.

The entry and exit orders of vehicle i are given by

$$\theta_i(r_i) = N(0, r_i) = N_0 + F(r_i) = i, \tag{18}$$

$$\theta_i(s_i) = N(l, s_i) = G(s_i). \tag{19}$$

Here we use a vehicle's entry order as its ID. Clearly $\theta_i(t) = \theta_i(r_i) = \theta_i(s_i)$ is constant for any vehicle i if and only if all vehicles follow the FIFO principle. We further define the order change, M_i, as

$$M_i = \theta_i(s_i) - \theta_i(r_i) = G(s_i) - N_0 - F(r_i), \tag{20}$$

which is positive if it is slower than the average traffic and negative if it is faster.

From the definition in (16), we have the change in vehicle i's order as

$$\frac{\mathrm{d}}{\mathrm{d}t}\theta_i(t) = -k\left(X_i(t), t\right)\frac{\mathrm{d}}{\mathrm{d}t}X_i(t) + q\left(X_i(t), t\right) = k\left(X_i(t), t\right)\left(v\left(X_i(t), t\right) - v_i(t)\right), \tag{21}$$

where $v_i(t)$ is vehicle i's speed at t, and $v(x, t)$ is the average speed of the total traffic stream at x and t. Therefore, a vehicle follows the FIFO principle if and only if its order remains constant, or equivalently, if and only if its speed equals the average speed.

Furthermore, a vehicle gains its order if it is slower, and loses its order otherwise. If $\theta_i(t_1) > \theta_j(t_1)$ but $\theta_i(t_2) < \theta_j(t_2)$ for $t_2 > t_1$, then vehicle i overtakes vehicle j between t_1 and t_2. Thus, the new variable, $\theta_i(t)$, can capture FIFO violation. Note that the vehicle order variable only describes the overtaking phenomenon but not the underlying lane change or other related overtaking mechanism.

3.2. An extension of Newell's model

We denote $X_i^1(t)$ and $X_i^2(t)$ as the respective inverse functions of $N_1(x, t)$ and $N_2(x, t)$; i.e., $X_i^1(t)$ satisfies

$$N_1\left(X_i^1(t), t\right) = F\left(t - \frac{X_i^1(t)}{V}\right) + N_0 = \theta_i(t), \tag{22}$$

and $X_i^2(t)$ satisfies

$$N_2\left(X_i^2(t), t\right) = G\left(t - \frac{l - X_i^2(t)}{W}\right) + \left(l - X_i^2(t)\right)K = \theta_i(t). \tag{23}$$

Equivalently, we have

$$X_i^1(t) = X_1(\theta_i(t), t), \quad X_i^2(t) = X_2(\theta_i(t), t). \tag{24}$$

Theorem 2.3 directly leads to the following theorem.

Theorem 3.1. *At t, the location of the ith vehicle on the road segment, $X_i(t)$, is given by*

$$X_i(t) = \min\{X_i^1(t), X_i^2(t)\}. \tag{25}$$

Proof. From the definitions of $X_i(t) = X(\theta_i(t), t)$, $X_i^1(t) = X_1(\theta_i(t), t)$, and $X_i^2(t) = X_2(\theta_i(t), t)$, (15) directly leads to (25) if we substitute n by $\theta_i(t)$ in the former. □

(25) is based on but an extension of Newell's simplified kinematic wave model in the Lagrangian coordinates, since the independent variable is time t and vehicle ID i. Newell model in (11) calculates the cumulative flow, $N(x, t)$, at a location, x, inside a road segment; the new model in (25) calculates the location, $X(n, t)$, of a cumulative flow, n. Thus they are equivalent when we focus on the aggregate traffic flow. However, in the new model in (25), we further introduce $n = \theta_i(t)$ for individual vehicle i, from which we can obtain $X_i(t) = X(\theta_i(t), t)$. Therefore the new model is equivalent to Newells model at the aggregate level but considers individual vehicles overtaking behaviors.

Note that this formulation is different from Newell's simplified car-following model (Newell, 2002), which is also in the Lagrangian coordinates: (i) In the car-following model a vehicle's trajectory is determined by its leader's trajectory, but by the boundary cumulative flows in (25); (ii) more importantly the FIFO principle is always observed in the car-following model, but not necessarily in (25). These unique features make the new formulation, (25), a suitable model for estimating vehicles' trajectories from the boundary cumulative flows and vehicles' entry and exit times.

4. Two algorithms for estimation of vehicle trajectories

In this section we present two estimation algorithms based on the new formulation of Newell's simplified kinematic wave model, (25), depending on whether the vehicle trajectories follow the FIFO principle or not.

4.1. Estimation of FIFO trajectories

When vehicles follow the FIFO principle, the trajectory of vehicle i establishes a contour line of the function $N(x, t)$, as shown in

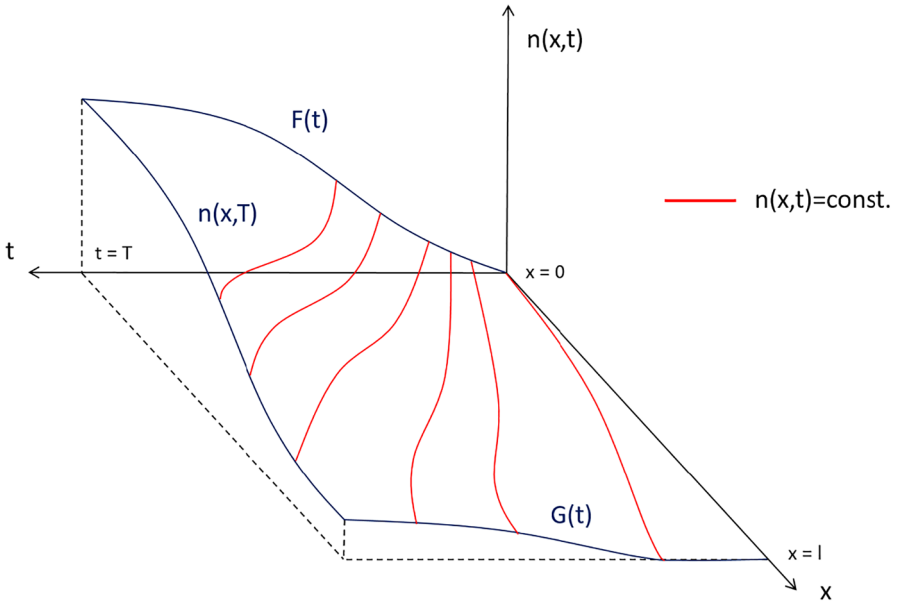

Fig. 3. Estimation of FIFO trajectories.

Fig. 3. In this case, vehicle i's order at any time is constant at θ_i. There are three simple choices of θ_i: (i) $\theta_i = \theta_i(r_i) = i$; i.e., vehicle i's order is always its entry order; (ii) $\theta_i = \theta_i(s_i)$; i.e., vehicle i's order is always its exit order; or (iii)

$$\theta_i = \frac{\theta_i(r_i) + \theta_i(s_i)}{2}; \tag{26}$$

vehicle i's order is always the average of its entry and exit orders. Among the three choices, (26) is the best as it uses all available information. Thus we use it as vehicle i's order when estimating its FIFO trajectory. Note that, however, (26) has a limitation in the sense that two vehicles with totally different entry and exit orders could have the same estimated trajectories: for example, a vehicle with entry order 1 and exit order 3 would have the same θ_i as a vehicle with entry order 3 and exit order 1. Theorem 3.1 can be directly applied to estimate a vehicle's trajectory with $X_i^1(t)$ and $X_i^2(t)$ defined as follows:

$$F\left(t - \frac{X_i^1(t)}{V}\right) + N_0 = \theta_i,$$
$$G\left(t - \frac{l - X_i^2(t)}{W}\right) + \left(l - X_i^2(t)\right)K = \theta_i.$$

With observed cumulative flows $F(t)$ and $G(t)$, together with estimated values of N_0, V, W and K in Sun et al. (2017), we can estimate vehicle i's trajectory in the following steps:

- Divide the time interval $[r_i, s_i]$ into time steps of size $\Delta t = 0.1sec$ (NGSIM time-step size).
- Compute the location of vehicle i at $t = m\Delta t$, where $m\Delta t \in [r_i, s_i]$, in the uncongested case, $X_i^1(m\Delta t)$:

$$X_i^1(m\Delta t) = [m\Delta t - F^{-1}(\theta_i - N_0)]\cdot V.$$

- Compute the location of vehicle i in the congested case, $X_i^2(m\Delta t)$:

$$G\left(m\Delta t - \frac{l - X_i^2(m\Delta t)}{W}\right) + K\left(l - X_i^2\left(m\Delta t\right)\right) - \theta_i = 0,$$

  which can be calculated with a bisection method or other methods.
- Take the minimum of both locations to obtain the actual location

$$X_i(m\Delta t) = \min\{X_i^1(m\Delta t), X_i^2(m\Delta t)\}. \tag{27}$$

4.2. Estimation of non-FIFO trajectories

In reality, vehicles usually violate the FIFO principle on a multi-lane road, even in relatively stationary traffic conditions. That is, the order change, M_i, is usually non-zero. In this section, we present a method to take into account the order gain for a vehicle when estimating its trajectory.

Here we assume that the order change of vehicle i, M_i, is achieved uniformly during its time interval on the road segment, $[r_i, s_i]$. Thus we can introduce the following linear order-changing model:

$$\theta_i(t) = a_i t + b_i. \tag{28}$$

From (21), we can see that the linear order-changing model is approximately true in nearly steady traffic when $k(x, t) \approx k$, $v(x, t) \approx v$, and $v_i(t) \approx v_i$ are all relatively constant, but $v_i(t)$ may not equal $v(x, t)$. In this case,

$$a_i \approx k(v - v_i),$$

which is also the rate of flow overtaking vehicle i.

Note that the order-changing function should be a staircase function in reality, but we can approximate it by a linear function. From (18) and (19), we can simplify (28) as

$$\theta_i(t) = a_i(t - r_i) + N_0 + F(r_i), \tag{29}$$

where

$$a_i = \frac{M_i}{s_i - r_i}. \tag{30}$$

When the coefficient $a_i > 0$, the vehicle is gaining its order and driving slower than others; when $a_i < 0$, it is losing its order and driving faster than others. Therefore, a_i can be related to the type of a vehicle, a driver's aggressiveness, and other characteristics. But a comprehensive study on the relationship between the characteristics of a driver-vehicle unit and the coefficient of the order-changing model is beyond the scope of this study.

With calculated order-changing model, (29), we can apply Theorem 3.1 to estimate a vehicle's trajectory with $X_i^1(t)$ and $X_i^2(t)$ defined as follows:

$$F\left(t - \frac{X_i^1(t)}{V}\right) + N_0 = \frac{M_i}{s_i - r_i}\left(t - r_i\right) + N_0 + F(r_i),$$
$$G\left(t - \frac{l - X_i^2(t)}{W}\right) + \left(l - X_i^2(t)\right)K = \frac{M_i}{s_i - r_i}\left(t - r_i\right) + N_0 + F(r_i).$$

With observed cumulative flows $F(t)$ and $G(t)$ as well as the order change M_i, together with estimated values of N_0, V, W and K in (Sun et al. (2017), we can estimate vehicle i's trajectory in the following steps:

- Calculate the coefficient a_i from (30).
- Divide the time interval $[r_i, s_i]$ into time steps of size $\Delta t = 0.1sec$.
- At $t = m\Delta t$, where $m\Delta t \in [r_i, s_i]$, calculate $\theta_i(m\Delta t)$ from (29).
- Compute the location of vehicle i in the uncongested case, $X_i^1(m\Delta t)$:

$$X_i^1(m\Delta t) = [m\Delta t - F^{-1}(\theta_i(m\Delta t) - N_0)]\cdot V.$$

- Compute the location of vehicle i in the congested case, $X_i^2(m\Delta t)$:

$$G\left(m\Delta t - \frac{l - X_i^2(m\Delta t)}{W}\right) + \left(l - X_i^2\left(m\Delta t\right)\right)K - \theta_i\left(m\Delta t\right) = 0,$$

  which can be calculated with a bisection method.
- Take the minimum of both locations to obtain the actual location

$$X_i(m\Delta t) = \min\{X_i^1(m\Delta t), X_i^2(m\Delta t)\}. \tag{31}$$

5. An empirical study

In this section, we implement the proposed two algorithms to estimate vehicles' trajectories and compare their performance with NGSIM datasets, which consist of the trajectories of vehicles traveling on a stretch of freeway between the Ventura Blvd and the Cahuenga Blvd off-ramps on the southbound US 101 freeway in Los Angeles, CA, as shown in Fig. 4, from 7:50 AM to 8:35 AM on June 15, 2005. The road segment is about 0.13 miles long with five regular lanes and one auxiliary lane. On average, it takes around 25 s for vehicles to go through this segment in congestion. The 45-min period is split into three 15-min intervals. A 2-min warm-up

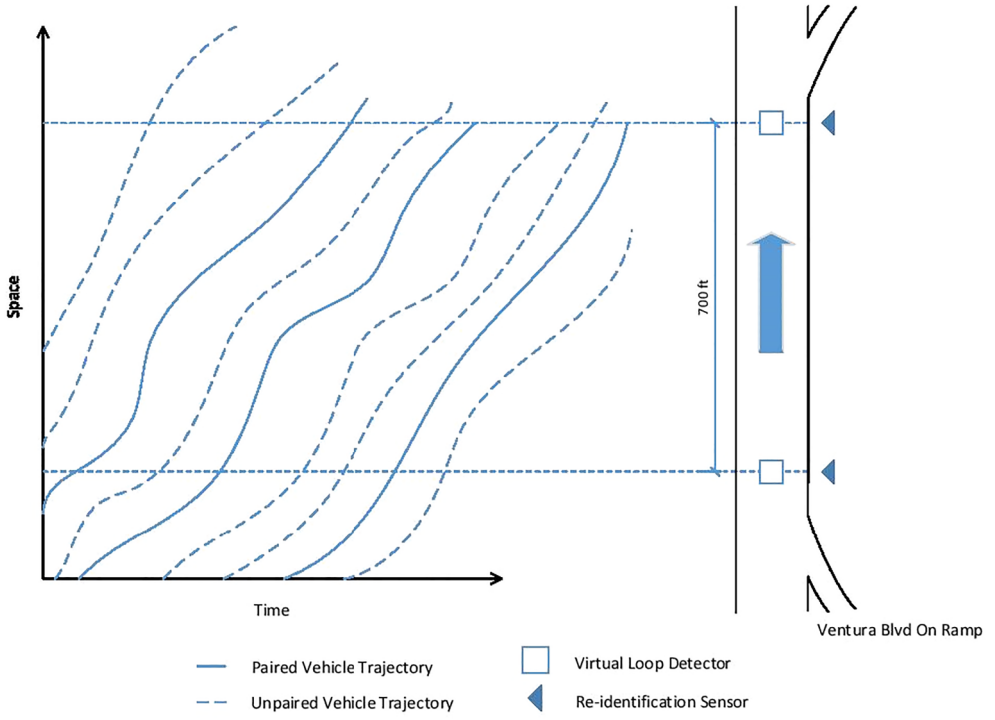

Fig. 4. Illustration of the Study Site.

period is used to ensure that all vehicle trajectories in the segment are tracked in the dataset. There are 1894 vehicle trajectories in the first time period, 1842 in the second and 1698 in the third. We deploy virtual loop detectors at both boundaries of the road segment and convert trajectory data into cumulative counts at these locations as well as vehicles' entry and exit times, from which vehicles' orders and order changes can be calculated.

5.1. Data Preparation

The sampling frequency of the NGSIM datasets is 10 Hz. Thus we set the time step-size $\Delta t = 0.1s$. For vehicle i, its location at time step j is $X_i(j\Delta t)$, which is given in the dataset. But in this study we assume that only the entry and exit times are known, and the whole trajectory is to be estimated. Then the ground-truth trajectories are used to quantify the accuracy of the estimation algorithms.

For vehicle i, we assume that the vehicle reidentification method can provide us the accurate entry/exit times of individual vehicles on the study site. In this study, these times are calculated from a vehicle's trajectory as follows. Let x_0 and x_l denote the entry and exit points of the segment respectively. We used a linear interpolation function to find the entry time r_i, formally,

$$r_i = j\Delta t + \frac{x_0 - X_i(j\Delta t)}{X_i(j\Delta t + \Delta t) - X_i(j\Delta t)}\Delta t,$$

where j satisfies $X_i(j\Delta t) \leqslant x_0 \leqslant X_i(j\Delta t + \Delta t)$. Similarly, the exit time is

$$s_i = j'\Delta t + \frac{x_l - X_i(j'\Delta t)}{X_i(j'\Delta t + \Delta t) - X_i(j'\Delta t)}\Delta t,$$

where j' is chosen such that $X_i(j'\Delta t) \leqslant x_l \leqslant X_i(j'\Delta t + \Delta t)$.

The cumulative counts $F(t)$ and $G(t)$ are practically step functions. Here we approximate them with piecewise linear functions passing through the crests, as illustrated in 5. In the plot, the cumulative counts at the upstream, $F(t)$, are approximated by $\widetilde{F}(t)$. In addition, the order change of vehicle i can be calculated from $M_i = G(s_i) - F(r_i) - N_0$.

As for the parameters (V, W, K) in the fundamental diagram and the initial number of vehicles N_0, we will use the estimations given by Sun et al. (2017) in each of the three time intervals in which the NGSIM dataset is divided. The values of these parameters are summarized in Table 2.

5.2. Results

In Fig. 6 we can compare the observed trajectories and the estimated trajectories with or without overtaking for vehicle 1130 in the third dataset. From the figure, we can see that without overtaking effects the vehicle would enter the road segment about 5 s later

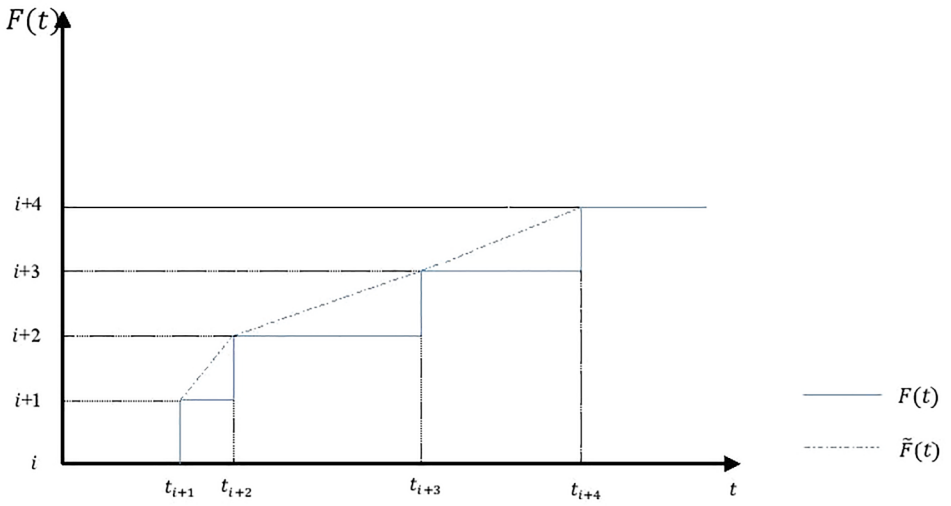

Fig. 5. Linear Approximation of Cumulative Flow.

Table 2
Parameters for Newell's model

Time interval	N_0(veh)	V(mph)	W(mph)	K (vpm)
7:50 AM - 8:05 AM	39	62.00	20.00	156.51
8:05 AM - 8:20 AM	39	50.00	25.67	141.46
8:20 AM - 8:35 AM	51	47.00	21.15	157.98

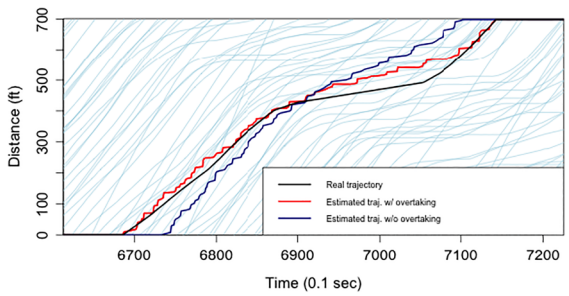

Fig. 6. Example of trajectory estimation.

and exit the road segment about 4 s earlier. But in reality its order is increased by 22; i.e., it is overtaken by 22 vehicles. From the figure we can see that the second algorithm with overtaking effects yields better estimated trajectory.

To examine the performance of the estimation algorithms, the estimated trajectories are compared with the real trajectories, given in the NGSIM datasets. The estimation error for each vehicle i is defined by the difference between the estimated and observed cumulative trajectories:

$$ERROR_i = \frac{A_{1i}}{A_{2i}} = \frac{\int_{r_i}^{s_i} \left| X_i(t) - \widehat{X}_i(t) \right| \mathrm{d}t}{\int_{r_i}^{s_i} \left| \widehat{X}_i(t) \right| \mathrm{d}t} \approx \frac{\sum_{j=r_i/\Delta t}^{s_i/\Delta t} \left| X_i\left(j\Delta t\right) - \widehat{X}_i\left(j\Delta t\right) \right|}{\sum_{j=r_i/\Delta t}^{s_i/\Delta t} \left| \widehat{X}_i\left(j\Delta t\right) \right|}, \tag{32}$$

where $X_i(t)$ represents the estimated location of vehicle i at time t and $\widehat{X}_i(t)$ is the observed location of the vehicle at that time. In Fig. 7 we illustrate the calculation of A_{1i} and A_{2i}. Clearly the error equals zero when the two trajectories overlap, and larger errors suggest larger differences between the two trajectories. The error defined in (32) is an extension of the relative error; this can be seen by removing the summation signs from both the numerator and denominator. Such a relative error can be used to compare the estimation performance of different vehicle trajectories. In contrast, the RMSE (root-mean-square error (RMSE) and errors in other norms are absolute average errors, which cannot be used to compare the estimation performance of different vehicle trajectories.

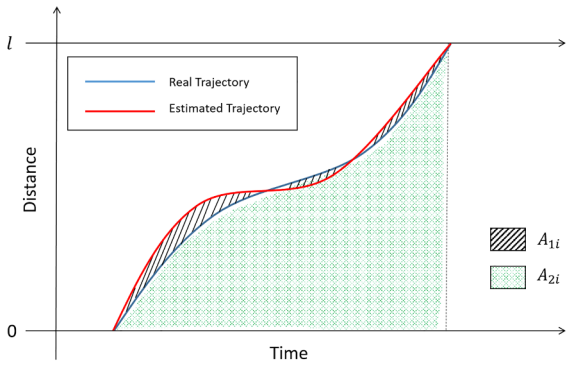

Fig. 7. Areas used to define the estimation error.

For example, for the vehicle shown in Fig. 6, the estimation error is 5.56% in the second algorithm, and 14.98% in the first algorithm. For vehicle i, we denote the ratio of the first algorithm's error to the second algorithm's error by η_i. Then in Fig. 8, we demonstrate the relationship between η_i and M_i. From the figure we can see that the greater the order change, the greater the difference between the estimated trajectories with and without FIFO assumption. Therefore it is important to consider the overtaking effects when estimating vehicles' trajectories.

Figs. 9–11 show the distributions of the estimation errors with the two algorithms for the three datasets. From the figures, we can see that the second algorithm outperforms the first one for all three datasets, since the estimation errors from the second algorithm are more clustered to the left, smaller values. To have a better interpretation, the distribution of errors can be approximated by a gamma distribution curve, which can be characterized by two parameters: the shape parameter α and the scale parameter β. They can be calculated from the mean μ and the standard deviation σ of errors according to the following relationships:

$$\alpha = \left(\frac{\mu}{\sigma}\right)^2 \tag{33}$$

and

$$\beta = \frac{\sigma^2}{\mu}. \tag{34}$$

The values of α and β obtained for the distributions plotted in Figs. 9–11 are contained in Table 3.

In Table 4, we further summarize the estimation errors for the three datasets with the two algorithms. The variables are defined as follows:

- $\bar{v}$: Average speed of the vehicles;
- $\sigma(v)$: Standard deviation of the speeds along the road segment;
- $\bar{E_1}$: Average estimation error with the first algorithm without overtaking effects;
- $\sigma(E_1)$: Standard deviation of the estimation errors with the first algorithm;
- $\bar{E_2}$: Average estimation error with the second algorithm with overtaking effects;
- $\sigma(E_2)$: Standard deviation of the estimation errors with the second algorithm.

From Table 4 we can see that the average estimation error is significantly lower with the second algorithm: the average estimation error is over 13% with the first algorithm, but below 10% with the second. In addition, the standard deviation of the estimation errors is also smaller with the second algorithm. This further confirms that the second algorithm with overtaking effects is more accurate and reliable.

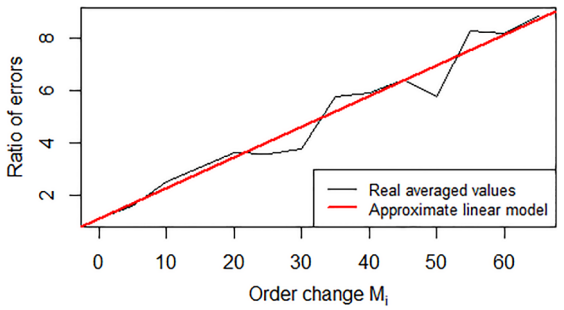

Fig. 8. Relationship between the ratio of errors in both algorithms and order change.

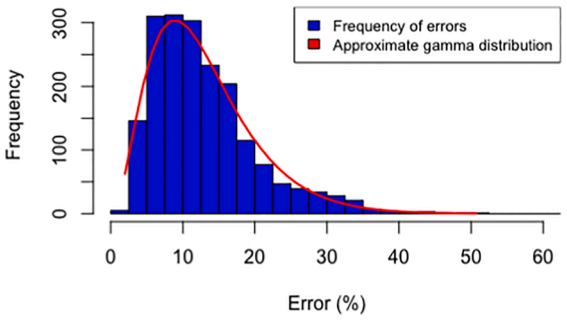

(a) The first algorithm without overtaking

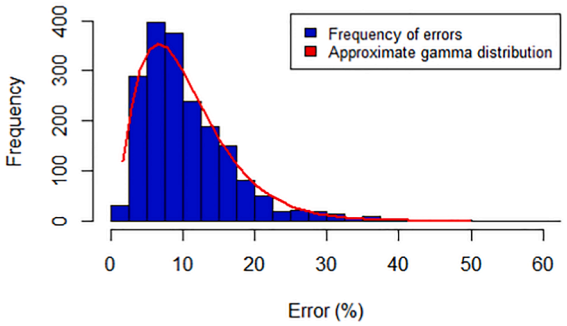

(b) The second algorithm with overtaking

Fig. 9. Distribution of the estimation errors in Dataset 1.

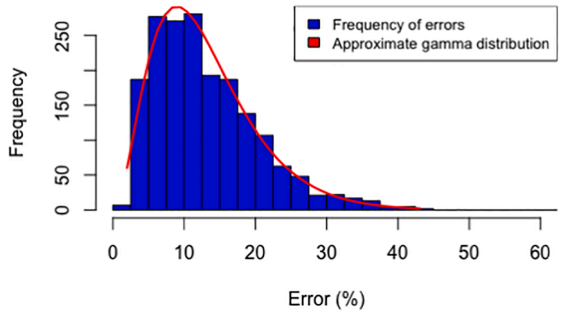

(a) The first algorithm without overtaking

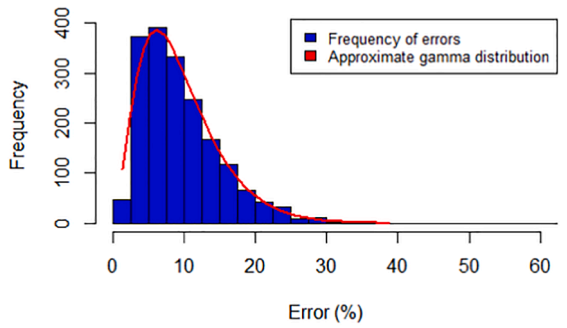

(b) The second algorithm with overtaking

Fig. 10. Distribution of the estimation errors in Dataset 2.

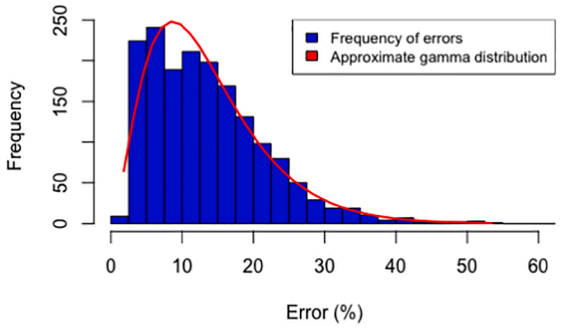

(a) The first algorithm without overtaking

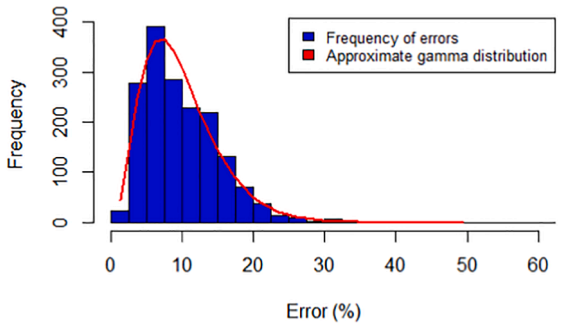

(b) The second algorithm with overtaking

Fig. 11. Distribution of the estimation errors in Dataset 3.

Table 3
Parameters of the Gamma Distributions

Dataset	Algorithm	α	β
1	FIFO	3.20	4.04
	Overtaking	2.70	3.89
2	FIFO	3.18	4.10
	Overtaking	2.82	3.38
3	FIFO	2.76	4.91
	Overtaking	3.48	2.84

Table 4
Estimation errors for the three datasets with the two algorithms

Dataset	$\bar{v}$(ft/s)	$\sigma(v)$	$\bar{E_1}$(%)	$\sigma(E_1)$	$\bar{E_2}$(%)	$\sigma(E_2)$
1	37.918	12.332	12.90	7.22	10.52	6.40
2	33.001	11.177	13.06	7.32	9.53	5.68
3	27.825	9.419	13.54	8.15	9.88	5.30

In Fig. 12 we show the distribution of the parameter a_i for all vehicles in the three datasets, which can be considered a measure of drivers' aggressiveness. The distribution can be approximated by a normal distribution with a mean of about 0. From the figure we can observe a high percentage of values very close to 0, and this suggests that most of the vehicles do not change their orders in congested traffic. However, the comparison between the two estimation algorithms suggests that the small percentage of vehicles with substantial order changes can actually significantly impact the estimation accuracy.

6. Conclusions

In this study we first reviewed Newell's simplified kinematic wave model and presented two lemmas regarding its property. After

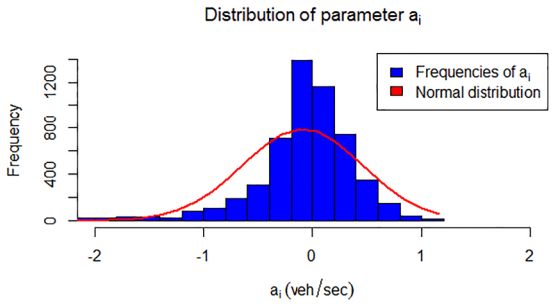

Fig. 12. Distribution of the parameter a_i for all the vehicles.

defining a new variable for vehicle orders, we derived based on Newell's model a new kinematic wave model in the Lagrangian coordinates to calculate a vehicle's trajectory from its order given at a time instant. The new kinematic wave model, (25) and (29), is consistent at the aggregate level with Newell's simplified kinematic wave model and, therefore, the LWR model, but allows for FIFO violation among individual vehicles. Then with the new model we proposed two algorithms for estimating vehicles' trajectories on a road segment from the boundary cumulative flows and vehicles' orders at the two boundaries: the first algorithm assuming the first-in-first-out (FIFO) principle, but the second one considering the overtaking effects. With three NGSIM datasets, we carefully compared the two algorithms and found that the second one is more accurate (10% vs 13% in the estimation errors) and reliable. This verifies the advantage of incorporating FIFO violation in the new model.

The new kinematic wave model has the following three novel components. First, it is in the Lagrangian coordinates but with Eulerian boundary conditions. Second, the model incorporates the overtaking effects through a new variable (vehicle order) in vehicles' orders. Finally, a linear model of order change was introduced in (29) to account for the change in vehicles' relative orders due to overtaking effects. The method for estimating vehicles' trajectories is based on the new model and, therefore, novel. In addition, we demonstrate that the new method is more accurate and reliable than the standard method with FIFO.

In our study, Newells model is one of the basic assumption, as the new model in (25) was directly derived from Newells model in (11). Another basic assumption is that the overtaking of vehicles is captured by the vehicle order variable in (16); in particular, we assume that the vehicle order is a linear function in time as shown in (29). Therefore, the consistency between the new model and Newells model is inherent. As an indication of such consistency, the parameters, N_0, V, W and K, were estimated based on Newells model as in Sun et al. (2017).

Even with the second algorithm with overtaking effects, there are other possible error sources that contribute to the estimation errors: low accuracy in the set of parameters (V, W, K) used, wrong trajectories recorded in the NGSIM datasets, and peak flows that cause the cumulative functions $F(t)$ and $G(t)$ to grow faster than the theoretical capacity of the road, making the estimated trajectories look less smooth. In addition, the linear order changing model is also an approximation. How to further account for these errors is subject to future studies. For example, for freeways with HOV lanes, where different lanes have different speeds that lead to FIFO violation, the method still applies, as long as all the lanes are approximately unifiable; i.e., as long as Newell's model applies to the total traffic. But the estimation accuracy depends on that of the individual assumptions on Newell's model and the vehicle order function.

Note that the estimated trajectories in Fig. 6 are non-differentiable; they are caused by piecewise linear, non-differential cumulative flows, as shown in Fig. 5. In applications, such non-smoothness can be readily fixed by applying standard smoothing methods, including the moving average, Savitzky-Golay, and other methods. Please note again that this study focuses on the methodology for estimating vehicle trajectories with the new kinematic wave model. Thus we choose to use the non-smooth estimated trajectories to evaluate the performance of the estimation methods.

Besides, the following are more suggested directions for further research in the topic:

- developing an iterative method for better estimating the parameters (V, W, K) with observed vehicle trajectories,
- trying different order change functions $\theta_i(t)$ to obtain better estimation in vehicle trajectories,
- extending the current method to accommodate other data types (for example, GPS data, Bluetooth data),
- extending the new model in (25) to accommodate internal bottlenecks on a road segment,
- developing other methods to estimate non-FIFO vehicle trajectories, for example, based on the equivalent formulation of Newell's model, (11), in passing times, $T(n, x)$,
- and exploring other applications, including emission estimation and travel time estimation.

Acknowledgments

We would like to thank three anonymous reviewers for their insightful and constructive comments, which have helped to improve the presentation substantially.

References

Barrios, C., Motai, Y., 2011. Improving estimation of vehicle's trajectory using the latest global positioning system with kalman filtering. IEEE Trans. Instrum. Meas. 60 (12), 3747–3755.

Coifman, B., 2002. Estimating travel times and vehicle trajectories on freeways using dual loop detectors. Transp. Res. Part A 36 (4), 351–364.

Coifman, B., Cassidy, M., 2002. Vehicle reidentification and travel time measurement on congested freeways. Transp. Res. Part A 36 (10), 899–917.

Daganzo, C.F., 1997. Fundamentals of Transportation and Traffic Operations. Pergamon-Elsevier, Oxford, U.K.

Daganzo, C.F., 2005. A variational formulation of kinematic waves: basic theory and complex boundary conditions. Transp. Res. Part B 39 (2), 187–196.

Evans, L., 1998. Partial Differential Equations. American Mathematical Society.

Greenshields, B.D., 1935. A study of traffic capacity. Highway Research Board Proceedings 14, 448–477.

Haberman, R., 1977. Mathematical models.

Jeng, S.T., 2007. Real-time vehicle reidentification system for freeway performance measurements.

Jiang, Z., Chen, X.M., Ouyang, Y., 2017. Traffic state and emission estimation for urban expressways based on heterogeneous data. Transp. Res. Part D 53, 440–453.

Jin, W.-L., 2015. Continuous formulations and analytical properties of the link transmission model. Transp. Res. Part B 74, 88–103.

Jin, W.-L., 2016. On the equivalence between continuum and car-following models of traffic flow. Transp. Res. Part B 93, 543–559.

Jin, W.-L., 2017. Unifiable multi-commodity kinematic wave model. In: Transportation Research Procedia: Proceedings of the 22nd International Symposium on Transportation and Traffic Theory 23, pp. 137–156.

Jin, W.-L., Li, L., 2007. First-In-First-Out is violated in real traffic. In: Proceedings of Transportation Research Board Annual Meeting.

Jin, W.-L., Yan, Q., 2019. A formulation of unifiable multi-commodity kinematic wave model with relative speed ratios. Transp. Res. Part B 128, 236–253.

Jin, W.-L., Zhang, Y., Chu, L., 2006. Measuring first-in-first-out violation among vehicles. In: Proceedings of TRB Annual Meeting.

Laval, J.A., Leclercq, L., 2013. The Hamilton–Jacobi partial differential equation and the three representations of traffic flow. Transp. Res. Part B 52, 17–30.

Li, J., Perrine, K., Wu, L., Walton, C.M., 2019. Cross-validating traffic speed measurements from probe and stationary sensors through state reconstruction. Int. J. Transp. Sci. Technol.

Lighthill, M.J., Whitham, G.B., 1955. On kinematic waves: II. A theory of traffic flow on long crowded roads. Proc. Roy. Soc. London A 229 (1178), 317–345.

Mehran, B., Kuwahara, M., Naznin, F., 2012. Implementing kinematic wave theory to reconstruct vehicle trajectories from fixed and probe sensor data. Transp. Res. Part C 20 (1), 144–163.

Mo, B., Li, R., Zhan, X., 2017. Speed profile estimation using license plate recognition data. Transp. Res. Part C 82, 358–378.

Moskowitz, K., 1965. Discussion of 'freeway level of service as in uenced by volume and capacity characteristics' by D.R. Drew and C.J. Keese. Highway Res. Rec. 99, 43–44.

Munjal, P., Hsu, Y.S., Lawrence, R., 1971. Analysis and validation of lane-drop effects on multilane freeways. Transp. Res. 5 (4), 257–266.

Newell, G.F., 1993. A simplified theory of kinematic waves in highway traffic I: General theory. II: Queuing at freeway bottlenecks. III: Multi-destination flows. Transp. Res. Part B 27 (4), 281–313.

Newell, G.F., 2002. A simplified car-following theory: a lower order model. Transp. Res. Part B 36 (3), 195–205.

Oh, C., Ritchie, S.G., Jayakrishnan, R., 2002. Real-time origin-destination (od) estimation via anonymous vehicle tracking. IEEE Trans. Intell. Transp. Syst. 582–586.

Oh, C., Tok, A., Ritchie, S.G., 2005. Real-time freeway level of service using inductive-signature-based vehicle reidentification system. IEEE Trans. Intell. Transp. Syst. 6 (2), 138–146.

Ponsa, D., Lopez, A., 2007. Vehicle Trajectory Estimation Based on Monocular Vision Vol. 4477 Springer, Berlin Heidelberg.

Richards, P.I., 1956. Shock waves on the highway. Oper. Res. 4 (1), 42–51.

Seo, T., Byen, A.M., Kusakabe, T., Asakura, Y., 2017. Traffic state estimation on highway: a comprehensive survey. Annu. Rev. Control.

Sun, C., Ritchie, S.G., Tsai, K., Jayakrishnan, R., 1999. Use of vehicle signature analysis and lexicographic optimization for vehicle reidentification on freeways. Transp. Res. Part C 7 (4), 167–185.

Sun, Z., Ban, X.J., 2013. Vehicle trajectory reconstruction for signalized intersections using mobile traffic sensors. Transp. Res. Part C 36, 268–283.

Sun, Z., Hao, P., Ban, X.J., Yang, D., 2015. Trajectory-based vehicle energy/emissions estimation for signalized arterials using mobile sensing data. Transp. Res. Part D 34, 27–40.

Sun, Z., Jin, W.-L., Ritchie, S.G., 2017. Simultaneous estimation of states and parameters in Newell's simplified kinematic wave model with Eulerian and Lagrangian traffic data. Transp. Res. Part B 104, 106–122.

USDOT, 2008. Ngsim: Next generation simulation. <http://www.ngsim.fhwa.dot.gov>.

Wan, N., Vahidi, A., Luckow, A., 2016. Reconstructing maximum likelihood trajectory of probe vehicles between sparse updates. Transp. Res. Part C 65, 16–30.

Yan, Q., Jin, W.-L., 2017. Calibration and validation of non-fifo unifiable lane-based fundamental diagrams in a multi-lane traffic flow system. In: Transportation Research Board 96th Annual Meeting. No. 17-06632. Presented.

Yang, Q., Boriboonsomsin, K., Barth, M., 2011. Arterial roadway energy/emissions estimation using modal-based trajectory reconstruction. In: 14th International IEEE Conference on Intelligent Transportation Systems (ITSC). IEEE, pp. 809–814.